https://doi.org/10.3311/PPci.40107

Periodica Polytechnica Civil Engineering, 69(4), pp. 1063–1077, 2025

Strength Properties and Evaluation Method of Composite Modified Carbonaceous Mudstone Soil-rock Mixtures

Ling Zeng[1], Hui-Cong Yu[1,2], Wen-Guang Wang[3], Chao-Wei Xue[4], Wei Wen[1], Qian-Feng Gao[5*], Han-Bing Bian[2], Jin-Tao Luo[1], Jian-Ping Song[6], You-Jun Li[6]

[1] School of Civil and Enironmental Engineering, Changsha University of Science & Technology, Changsha 410114, China
[2] Laboratoire de Génie Civil et géo-Environnement, Université de Lille, IMT Nord Europe, Univ. Artois, JUNIA, ULR 4515-LGCgE, F-59000 Lille, France
[3] Guangxi Nanning Second Ring Expressway Co., Ltd., Nanning 530005, China
[4] Anhui Zhery Property Co., Ltd., Wuhu 241009, China
[5] School of Transportation, Changsha University of Science & Technology, Changsha 410114, China
[6] Guangxi Transportation Science and Technology Group Co., Ltd., Nanning 530007, China
* Corresponding author, e-mail: qianfeng.gao@csust.edu.cn

Received: 07 February 2025, Accepted: 19 August 2025, Published online: 25 August 2025

Abstract

The application of carbonaceous mudstone soil-stone mixtures (CM-SRM) in embankment engineering is limited due to its poor mechanical properties. This study aims to enhance the strength properties of CM-SRM by modifying it with guar gum, fly ash and red clay. Unconfined compressive strength (UCS) tests and triaxial compression tests were carried out using orthogonal design methods to systematically analyze the mechanical properties and modification mechanisms of modified CM-SRM. The results indicated that the modified CM-SRM exhibited failure modes such as single-shear, single-shear-bulging, double-shear, and double-shear-bulging, with fly ash and guar gum dosages significantly affecting both failure modes. Unconfined compressive strength and cohesion increased post-modification, with minor changes in friction angle. Orthogonal analysis reveals that guar gum dosage significantly effects on UCS and shear strength indexes, whereas the effect of fly ash is comparatively weaker. Based on the test results, a shear strength evaluation method based on linear and nonlinear models is proposed. The study shows that the composite modification mechanisms of red clay, fly ash, and guar gum on CM-SRM mainly includes bonding and filling effects, cation exchange, and gel aggregation. The suggested dosage combination is 10% red clay, 5% fly ash, and 4% guar gum.

Keywords

embankment filling, soil-rock mixture, carbonaceous mudstone, orthogonal test, strength properties

1 Introduction

With the rapid development of global infrastructure, the demand for embankment fillers has increased significantly. Carbonaceous mudstone is a soft rock rich in clay minerals, widely distributed in southwest China [1, 2]. Large amounts of waste carbonaceous mudstone are generated during highway construction excavations, and its use as embankment fill can effectively reduce construction costs and minimize environmental pollution [3, 4]. However, carbonaceous mudstone easily disintegrates and softens upon water exposure, showing low strength [5], which limits its direct engineering application. Improving the strength properties can advance the application of carbonaceous mudstone in sustainable infrastructure.

In recent years, modification methods have been widely used to treat weak geotechnical materials, and common modifiers are classified as inorganic and organic gelling materials. Inorganic gelling materials such as cement [6], lime [7] and gypsum [8] enhance shear strength through physicochemical bonding [9]. For example, Wu et al. [10] observed that a mixture of cement and metakaolin modification significantly improved soil strength and reduced water sensitivity. Zeng et al. [11] noted that cement had a greater effect on cohesion enhancement of disintegrated carbonaceous mudstone (DCM) than red clay and fly ash. Amulya et al. [12] found that alkaline solutions such as sodium hydroxide combined with fly ash or granulated blast

Cite this article as: Zeng, L., Yu, H. C., Wang, W. G., Xue, C. W., Wen, W., Gao, Q. F., Bian, H. B., Luo, J. T., Song, J. P., Li, Y. J. "Strength Properties and Evaluation Method of Composite Modified Carbonaceous Mudstone Soil-rock Mixtures", Periodica Polytechnica Civil Engineering, 69(4), pp. 1063–1077, 2025. https://doi.org/10.3311/PPci.40107

furnace slag improved the UCS, California Bearing Ratio, and durability of clays. However, while inorganic gelling materials significantly improve soil strength, their high rigidity and poor ductility easily lead to brittle failure and constrain adaptability under high-strain conditions. Organic materials such as gum Arabic [13], polyurea [14] and guar gum [15, 16] are flexible and improve the ductility of soils, making them more plastic during failure. Organic gelling materials enhance bonding through cross-linking structures, and although they help to improve soil ductility, the enhancement of shear strength is not as significant as that of inorganic gelling materials. Therefore, composite modification can increase the overall strength and ductility of the soil, and enhance structural stability and durability [17].

Current studies mainly use the same type of materials to modify carbonaceous mudstone [18–20], and usually apply to DCM without considering large particles. In practice, disintegration of carbonaceous mudstone with large particles requires high cost and time, while excessively large particles lead to poor gradation, adversely affecting engineering properties [21, 22]. Using modified carbonaceous mudstone soil-rock mixtures (CM-SRM) for embankment filling can effectively solve these problems, but limited studies currently examine the modification of CM-SRM. For this reason, using red clay, fly ash, and guar gum as modified materials, the UCS and triaxial compression tests were carried out by the orthogonal design method to analyze the failure mode, stress-strain characteristics, and shear strength of CM-SRM, and explore the composite modification mechanisms. A shear strength evaluation method of modified CM-SRM was proposed based on the test results, providing a scientific basis for the application of modified materials in highway engineering.

2 Test materials and methods

2.1 Test materials

2.1.1 Carbonaceous mudstone

The carbonaceous mudstone used for the tests was taken from an excavated slope of the Lantian Expressway in Guangxi, China, and particles with a size of less than 20 mm were sieved for subsequent tests. Firstly, X-ray diffraction (XRD) and X-ray fluorescence spectroscopy (XRF) were carried out to analyze the mineral and chemical composition of the carbonaceous mudstone. The results show that the main minerals are quartz, muscovite, kaolinite, illite and calcite, and the chemical composition is shown in Table 1. Studies have shown that carbonaceous mudstones typically have a particle size of less than 2 mm when fully disintegrated, and exhibit soil-like properties, and hence referred to as DCM [23]. Consequently, this study set 2 mm as the boundary between 'soil' and 'stone', with particles larger than 2 mm defined as 'stone'. Subsequently, the basic physical properties of the DCM were tested according to the Chinese technical specification (JTG 3430-2020) [24], with results shown in Table 2, revealing that the DCM qualifies as low liquid limit silt (ML).

A previous study [4] shows that CM-SRM exhibits good engineering performance at 96 % compaction and 60 % stone content, but its UCS is less than 400 kPa, which severely limits its application. Therefore, this study carried out modification tests under the same compaction condition and stone content to enhance the strength properties of CM-SRM. After the CM-SRM was prepared according to 60 % stone content, a particle gradation curve was obtained by carrying out a sieve test (shown in Fig. 1), and the maximum dry density of 2.29 g/cm³ and the optimum water content of 6.77 % of the CM-SRM were determined by compaction tests.

2.1.2 Modified materials

Red clay is widely distributed in Guangxi, Hunan, and other areas of southern China, and was mainly formed by carbonate rocks through red clayification, with a high liquid limit and high plasticity [25, 26]. To reduce transport costs and source materials locally, red clay for the test was collected from the slopes near the sampling site of carbonaceous mudstone. The red clay was air-dried, crushed, and processed through a 2 mm sieve, and the sieved portion was used as the modified material (see Fig. 2(a)). Its particle gradation curve is shown in Fig. 1, and its chemical composition and basic physical properties are shown in Tables 1 and 2. Based on the Chinese technical specification (JTG 3430-2020) [24], this red clay is a high liquid limit clay (CH), with the main chemical compositions of SiO_2, Al_2O_3 and Fe_2O_3.

Fly ash is a fine industrial waste with a large specific surface area, strong adsorption capacity and good pozzolanic activity, which is widely used as concrete admixture and soil modifier [27]. The fly ash used in the test was produced by Zhengzhou Huifeng New Materials Co. Ltd, with a particle size of less than 0.045 mm, and the main chemical compositions of SiO_2, Al_2O_3, Fe_2O_3 and CaO (see Table 1, Fig. 2(b)).

Guar gum is a natural polysaccharide polymer extracted from guar beans, which is a light-yellow powder (Fig. 2(c)), with good thickening properties and can be dissolved in water to form a gel [28]. Guar gum is widely used in food, petroleum, and papermaking due to its low cost, environmental friendliness, and stability in acidic and thermal conditions [29].

Table 1 Chemical composition (%)

Material	SiO_2	Al_2O_3	Fe_2O_3	CaO	MgO	K_2O	TiO_2	P_2O5	Na_2O	SO_3	Loss on ignition
DCM	52.9	21.7	6.7	3.9	2.1	1.9	1.4	1.1	—	—	8.3
Red clay	42.7	39.2	7.3	—	0.8	1.7	1.2	0.3	—	—	6.8
Fly ash	48.3	29.7	4.8	2.9	1.6	1.4	—	—	1.5	1.8	8.0

Table 2 Basic physical properties

Material	Specific gravity	Optimum water content (%)	Maximum dry density ($g \cdot cm^{-3}$)	Liquid limit (%)	Plastic limit (%)	Plasticity index
DCM	2.66	10.86	2.01	34.1	26.7	7.4
Red clay	2.71	23.57	1.61	55.3	28.2	27.1

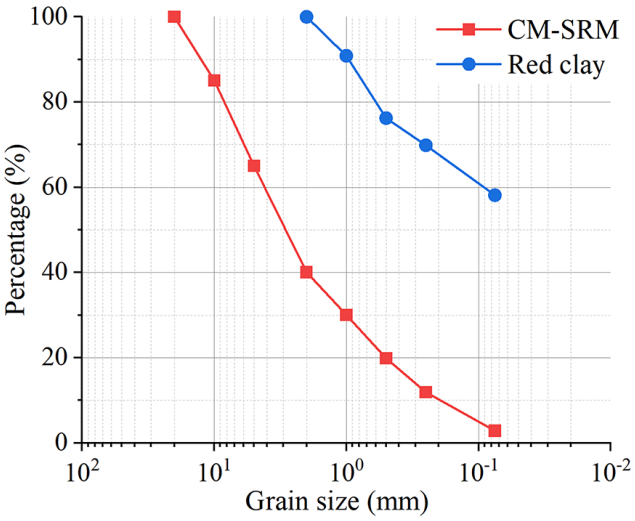

Fig. 1 Particle gradation curve

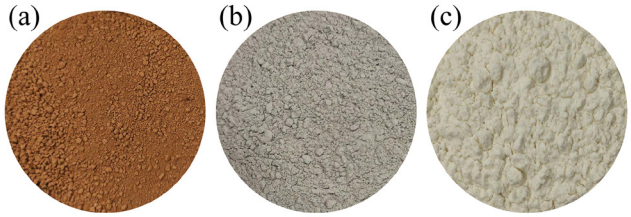

Fig. 2 Modified materials: (a) red clay, (b) fly ash, and (c) guar gum

2.2 Test methods

To investigate the strength properties of modified CM-SRM with different dosage levels, UCS tests and triaxial compression tests were carried out. Referring to the previous studies [11, 18, 30], four levels of red clay dosage of 0%, 5%, 10%, and 15%, fly ash dosage of 0%, 5%, 10%, and 15%, and guar gum dosage of 0%, 2%, 4%, and 6% were set. The orthogonal design is suitable for analyzing the effects of factors and their interactions on the experimental results due to its high efficiency in multifactor multilevel studies [31]. Therefore, this study used a three-factor, four-level orthogonal design method, and the test scheme is shown in Table 3.

Table 3 Orthogonal test scheme

Specimen	Red clay dosage (%)	Fly ash dosage (%)	Guar gum dosage (%)
T_1	0	0	0
T_2	0	5	2
T_3	0	10	4
T_4	0	15	6
T_5	5	0	2
T_6	5	5	0
T_7	5	10	6
T_8	5	15	4
T_9	10	0	4
T_{10}	10	5	6
T_{11}	10	10	0
T_{12}	10	15	2
T_{13}	15	0	6
T_{14}	15	5	4
T_{15}	15	10	2
T_{16}	15	15	0

2.2.1 Specimen preparation

Each specimen in this study was a cylindrical sample with a diameter of 100 mm and a height of 200 mm. The specimens were compacted to 96% density, with a 60% stone content and optimal water content of 10.86%. Firstly, the sieved dry soil material was weighed according to the percentage of each particle group in Fig. 1, and was uniformly mixed by adding modified material according to Table 3. Subsequently, pure water was added to the mixture, mixed uniformly and put into a sealed bag for 24 h, so that the water inside the soil material was uniformly distributed. Finally, the wet mixture was put into moulds and compacted in 5 layers by the static compaction method to obtain cylindrical specimens, which were cured indoors under natural conditions (20 °C ± 3 °C, relative humidity ≥ 50%) for 7 days for subsequent tests.

2.2.2 UCS tests

The tests used a WDW-20 universal testing machine, with strain-controlled loading at a rate of 1%·min^{-1}. During loading, axial force - axial strain curves were observed: if a peak appeared in the curve, loading continued for an additional 3%–5% strain until axial force stabilized; if no peak appeared, loading stopped at 16% axial strain.

2.2.3 Triaxial compression tests

The triaxial tests used an Autotriax Dynatriax 100/14 system from Controls (Italy) (Fig. 3), with modules for computer control, data acquisition, pneumatic pressure control, triaxial chamber, and actuator [32]. Tests were conducted under undrained and unconsolidated conditions at confining pressures σ_3 of 50 kPa, 100 kPa, and 150 kPa, with strain-controlled loading at 0.6%·min^{-1}. The loading stopping conditions were the same as those of the UCS tests.

3 Results and discussion

3.1 UCS properties of modified CM-SRMs

3.1.1 Failure modes

The failure mode of rock materials is closely related to their strength properties. Observation of the failure modes of the modified specimens under the unconfined condition with different modification schemes indicates four main failure modes: single-shear, single-shear-bulging, double-shear, and double-shear-bulging (Fig. 4) [33]. The unmodified CM-SRM exhibits a single-shear failure mode (Fig. 4(a)), where a distinct shear plane forms during compression, meaning low strength along the shear plane and weak structural integrity. For the low dosage of fly ash and guar gum conditions (e.g., T_6), the modified specimens still showed single-shear failure. With increased fly ash dosage (e.g., T_{11}, Fig. 4(c)), the failure mode of the modified specimen's changes to double-shear failure, i.e., with two planes of shear failure during the compression, meaning that the specimens have a more stable structure and higher shear strength. In addition, after guar gum addition, the modified specimens will bulge during the compression, resulting in single-shear-bulging (e.g., T_{13}, Fig. 4(b)) or double-shear-bulging (e.g., T_{15}, Fig. 4(d)) failure modes. Bulging may be caused by local stress concentration and strong plasticity of the material. Guar gum in the modified specimen can bind other particles to form aggregates, enhancing inter-particle bonding and overall plasticity, causing particle rearrangement and volume expansion of the specimen during the compression. However, the guar gum is unevenly distributed, and the strengths of carbonaceous mudstone particles and aggregates are different, leading to stress concentration and uneven bulging during compression.

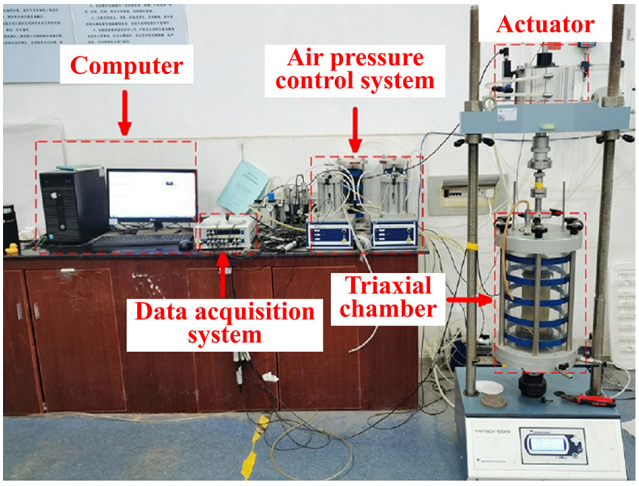

Fig. 3 Triaxial test system [32]

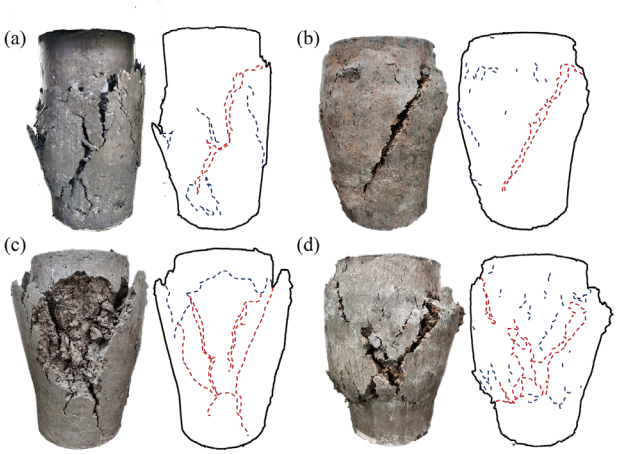

Fig. 4 Typical failure modes of specimens under unconfined conditions: (a) single-shear (T_0), (b) single-shear-bulging (T_{13}), (c) double-shear (T_{11}), and (d) double-shear-bulging (T_{15})

3.1.2 Stress-strain characteristics

Fig. 5 shows the stress-strain curves of specimens under the unconfined condition. Both modified and unmodified specimens exhibit an initial increase followed by a decrease in stress-strain curves, indicating strain-softening characteristics. The axial stress of unmodified specimens decreased rapidly after the peak of the stress-strain curve, and the strain softening effect is significant. In contrast, modified specimens show a slower rate of decrease in axial stress after the peak, and the strain softening effect is weak, particularly in the specimens without or with only 2% guar gum. The modified specimen with 15% red clay and 15% fly ash (T_{16}) exhibits the lowest strain softening, indicating the weakest brittleness characteristics.

Usually, the peak of the stress-strain curve corresponds to the compressive strength (UCS) and the failure strain of

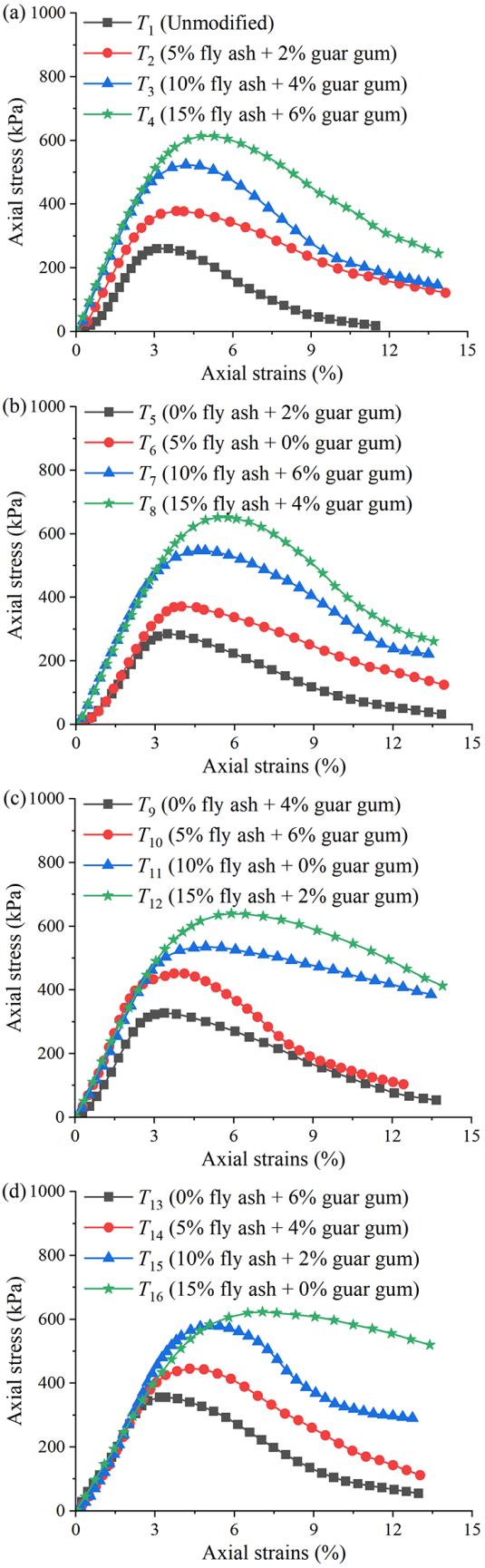

Fig. 5 Stress-strain curve: (a) 0% red clay, (b) 5% red clay, (c) 10% red clay, and (d) 15% red clay

the specimen, and Fig. 6 shows the test results of each specimen. The UCS of the unmodified specimen is 261.4 kPa and the failure strain is 3.2%, which means that it reaches the peak value at a small strain and shows high brittleness, and the strength decreases rapidly after the destruction, which is detrimental to structural safety. Both UCS and failure strain of the modified specimens increased, indicating that the addition of modified materials can effectively improve the strength and reduce the brittleness of CM-SRM. Among the specimens, the one modified with 5% red clay, 10% fly ash and 6% guar gum (T_7) shows the highest UCS of 652.1 kPa, which is an increase of 149.5%. While specimen T_{16} with 15% red clay, 15% fly ash and 0% guar gum shows the highest destructive strain of 6.8% with an increase of 112.5%. Additionally, with a constant red clay dosage, UCS increased with increasing guar gum dosage, while failure strain increased with increasing fly ash dosage.

3.1.3 Orthogonal analysis

For comparing the effect of different dosage levels on the UCS and failure strain of CM-SRM and assessing their

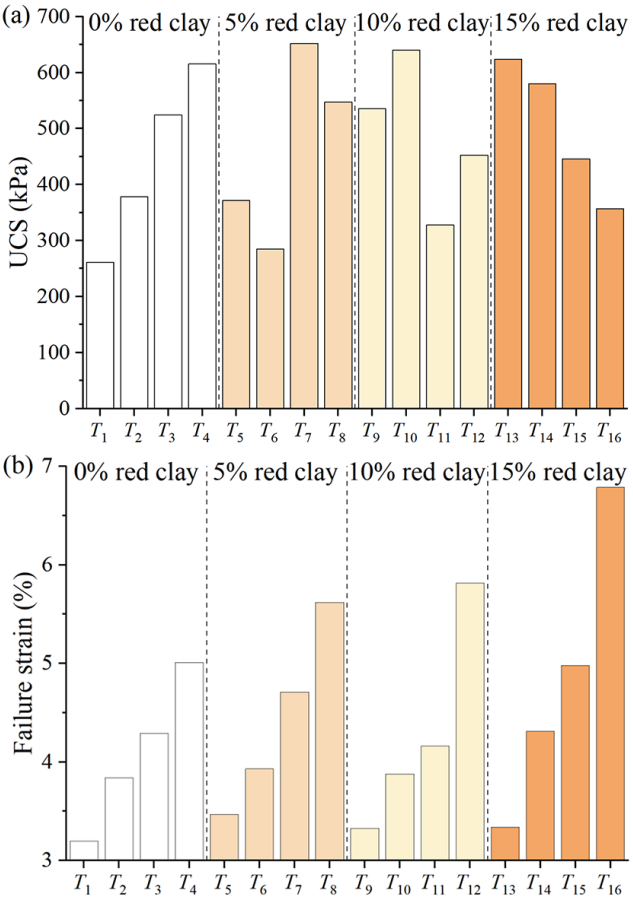

Fig. 6 UCS and failure strain of Modified CM-SRM: (a) UCS, and (b) failure strain

significance, range analysis and variance analysis were carried out, and the results are shown in Fig. 7 and Table 4, respectively. By comparing the mean values and range of UCS at different dosage levels (Fig. 7(a)), it is observed that the mean value of UCS increases gradually with the increase in the dosage of the three modified materials. Among them, the growth rate of UCS first rises then declines with the increase of red clay dosage, gradually decreases with fly ash dosage, and almost remains stable with the guar gum dosage. Range analysis indicates that the UCS variation due to guar gum is notably greater than that from fly ash and red clay, with red clay contributing slightly more than fly ash. Combined with the variance analysis (Table 4), the *p*-values of red clay, fly ash and guar gum are less than 0.05, suggesting significant effects of all three factors on UCS.

Fig. 7(b) shows that the mean failure strain is positively correlated with red clay and fly ash dosage, and negatively correlated with guar gum dosage. Both the rate and range of change in failure strain with fly ash content are greater than those of the other two modified materials. Combined with the results in Table 4, it can be seen that the effect of red clay and guar gum dosage on the failure strain is not significant, while only fly ash dosage has a significant effect.

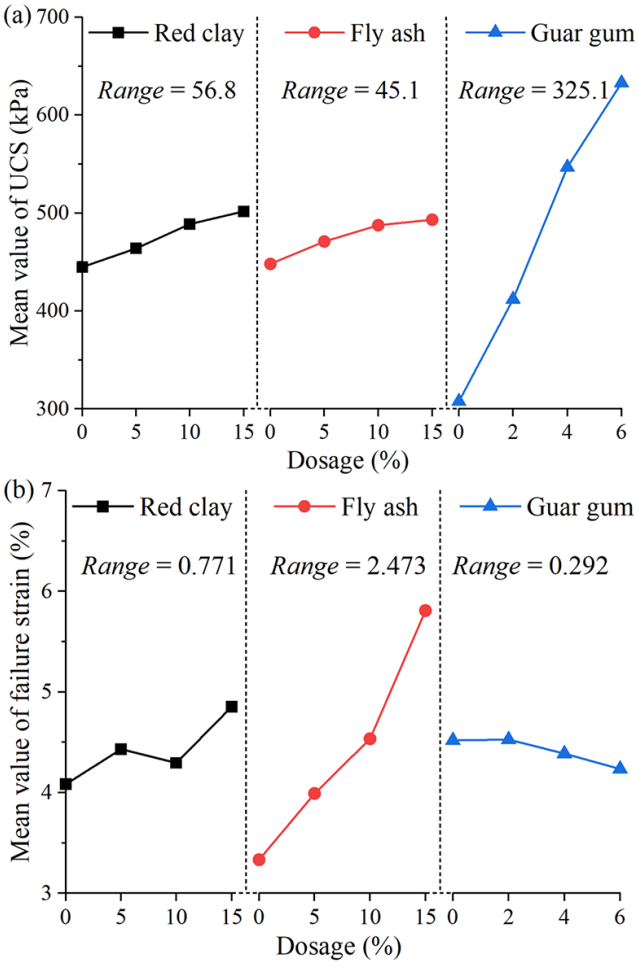

Fig. 7 Mean value of the test indexes at each dosage level: (a) UCS, and (b) failure strain

3.2 Shear strength properties of modified CM-SRMs

3.2.1 Failure modes

Under triaxial compression conditions, CM-SRMs showed four main failure modes: single-shear, single-shear-bulging, double-shear and double-shear-bulging, with a few specimens showing a single bulging failure. Fig. 8 illustrates the failure modes of some CM-SRMs (T_1, T_{10}, T_{15}) under triaxial compression conditions. Unmodified specimens display single-shear failure under both unconfined and triaxial compression conditions, with more pronounced failure as confining pressure increases. At σ_3 = 150 kPa, the unmodified specimens fractured completely along the shear plane, with a large number of particles spalling near the shear plane to make defects (Fig. 8(a)). Lateral confinement limited the lateral expansion and increased the internal stresses of the specimens, making them more susceptible to failure along the shear plane. As the confining pressure increases, the internal stress of the specimen may exceed the shear strength, leading to complete fracture along the shear plane and more significant failure. Modified specimens under 50 kPa confined pressure showed a different failure mode from that with unconfined conditions, mainly showing single-shear or double-shear failure without bulging. This may be attributed to lateral confinement, which also leads to a more uniform internal stress distribution, resulting in

Table 4 Variance analysis results for UCS and failure strain

Test index	Factor	Deviation sums of square	Mean square	*F* value	*p* value
UCS	Red clay dosage	7737.636	2579.212	16.020	0.003
	Fly ash dosage	4909.933	1636.644	10.166	0.009
	Guar gum dosage	248053.060	82684.353	513.574	0.001
Failure strain	Red clay dosage	1.270	0.423	3.414	0.094
	Fly ash dosage	13.196	4.399	35.465	0.001
	Guar gum dosage	0.226	0.075	0.607	0.635

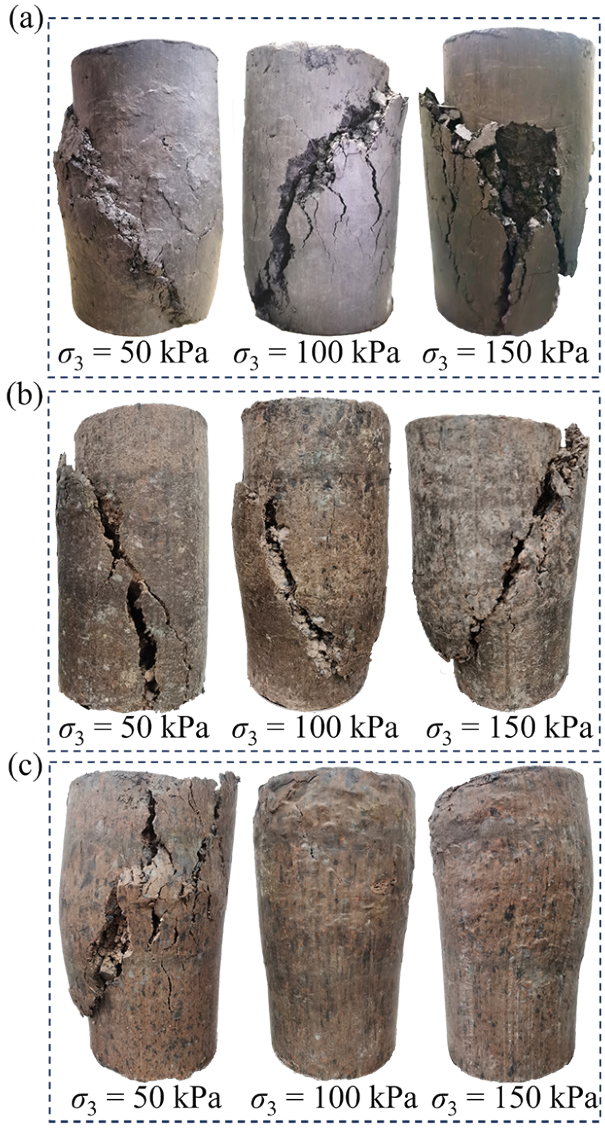

Fig. 8 Failure modes of specimens under triaxial compression conditions: (a) unmodified specimen (T_1), (b) modified specimen (T_{10}), and (c) modified specimen (T_{15})

shear stresses being concentrated on a single weak plane for most specimens, which exhibits single-shear failure. While double-shear failure occurs in some of the more stable structural specimens (Fig. 8(c)). With the increase of confining pressure, modified specimens gradually began to bulge (Fig. 8(b)), implying that the plasticity of modified specimens is significantly increased and stronger internal bonding. As shown in Fig. 8(c), modified specimen T_{15} showed only bulging under 100 kPa and 150 kPa of confining pressure without shear failure. This indicates that stress redistribution within the specimen under high confining pressure, with the material resisting stresses through plastic deformation, leads to higher overall strength and reduced stress concentration.

3.2.2 Shear strength indexes

Under triaxial conditions, the stress-strain curves of each specimen showed strain-softening characteristics. As axial strain increases, the deviation stress shows an obvious peak, after which it decreases rapidly and tends to stabilize gradually. Fig. 9 illustrates the stress-strain curves of unmodified specimen T_1 and modified specimen T_{15} under different confining pressures. It can be found that the curve shifts to the upper left as the confining pressure increases, the peak corresponding to the deviation stress increases, and the axial strain decreases, i.e., both strength and brittleness of specimens increase. Due to initial pores inside the specimen, the pore compression under the confining pressure makes the interparticle contact closer and restricts the lateral movement of the particles to a certain extent, which enhances the strength and brittleness, and this phenomenon is more significant in the modified specimen. Under the same confining pressure, modified specimens have larger deviation stresses and axial strains corresponding to the peak, reflecting greater strength and plasticity, consistent with results under unconfined conditions.

Based on the Mohr-Coulomb theory [34], the Mohr's circle of each specimen can be plotted. With the envelope of the Mohr's circle under different confining pressures, whose intercept is the cohesion c, and the slope is the tangent of the internal friction angle φ. As shown in Fig. 10, the cohesion of unmodified specimen T_1 is 39.63 kPa and the internal friction angle is 35.87°, while the cohesion of modified specimen T_{15} is increased to 95.45 kPa and the internal friction angle is 37.16°. Fig. 11 presents the cohesion and internal friction angle of the specimens under different modified schemes. Compared to unmodified

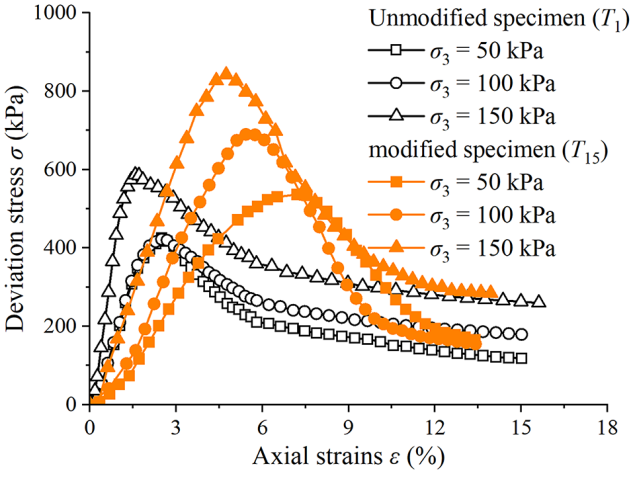

Fig. 9 Stress-strain curves of some specimens under triaxial compression conditions

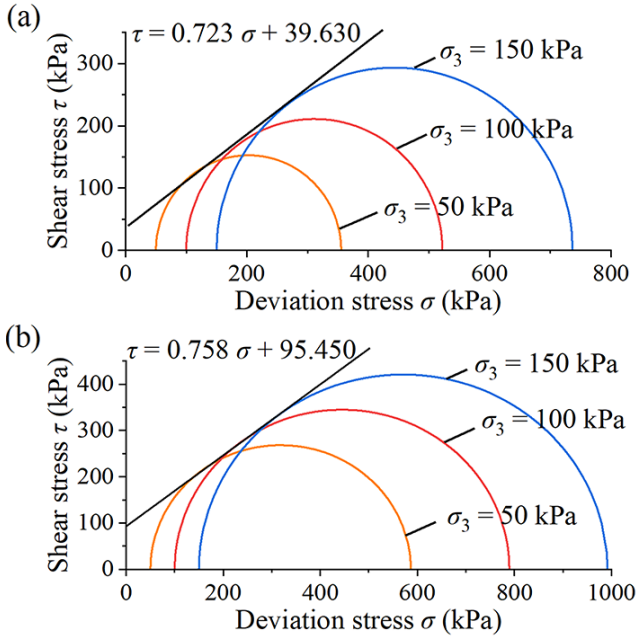

Fig. 10 Mohr's circles of some specimens: (a) T_1, and (b) T_{15}

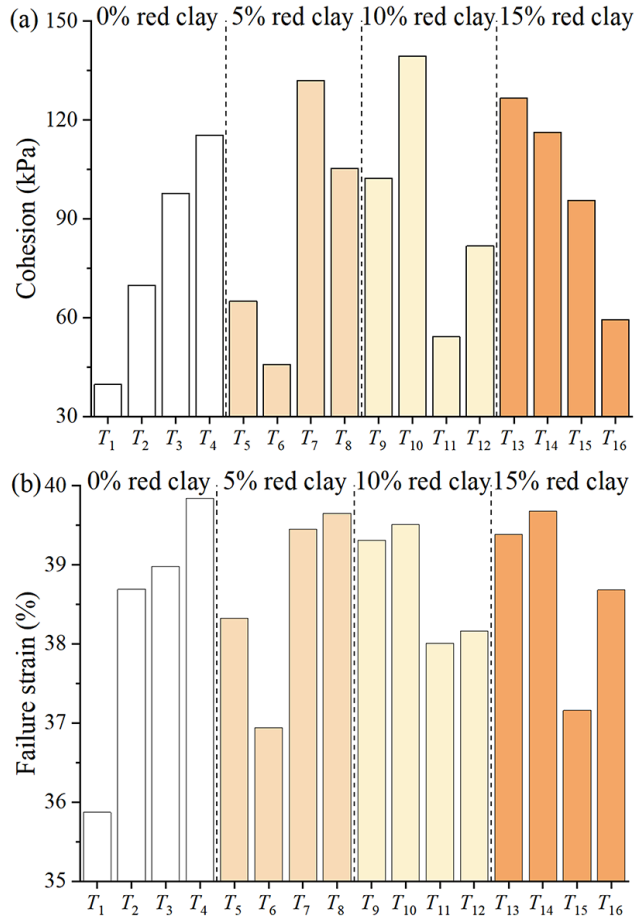

Fig. 11 Shear strength indexes of Modified CM-SRM: (a) cohesion, and (b) internal friction angle

specimens (T_1), modified specimens exhibit an increase in both cohesion and internal friction angle. Among them, with the largest increase in cohesion of 251.7% and the smallest of 15.4%, while internal friction angle increases are limited, with a maximum rise of 11.1%. Thus, the main effect of the modified material is to increase the cohesion of CM-SRM, which has less effect on the internal friction angle. With a constant red clay dosage, the cohesion of the specimens is positively correlated with the guar gum dosage (Fig. 11(a)), whereas there is no obvious pattern in the internal friction angle (Fig. 11(b)). When the guar gum dosage is fixed, cohesion of specimens is positively correlated with the red clay dosage (e.g., T_3, T_8, T_9, T_{14}), but specimens' cohesion decreases when the fly ash dosage is 0% (e.g., T_9).

Cohesion primarily consists of the original cohesion and the cured cohesion [35]. Guar gum can fill the voids between particles in CM-SRM and increase the contact area, thus improving the original cohesion. It also forms a gel that envelops soil particles into compact bonded aggregates, thereby enhancing the cured cohesion. Additionally, clay minerals in red clay adjust particle gradation, enabling closer particle contact and forming binding substances that create aggregates with loose particles, further improving both types of cohesion. Fly ash has fine particles and surface activity [36], which can fill fine voids and reduce water-soil interfacial tension, enhancing original cohesion. However, due to its poor bonding properties, increasing only fly ash content cannot greatly improve cohesion. While mixing red clay and guar gum, mixing fly ash can fill the small voids between the particles and make the particle structure more stable, thus effectively improving the original and curing cohesion. The internal friction angle is closely related to the interparticle friction and interlocking effects [37]. The bonding of red clay and guar gum enhances the friction and interlocking effect, but its water absorption reduces the lubrication effect, which in turn reduces the friction. Meanwhile, fly ash is tiny and spherical in shape, which can form a lubricating effect on the surface of the particles to reduce the friction. Thus, the combined effect of these materials slightly increases the internal friction angle, but with no clear pattern.

3.2.3 Orthogonal analysis

Fig. 12 shows the results of range analysis of cohesion and internal friction angle, with variance analysis results shown in Table 5. As shown in Fig. 12, the mean value of cohesion increased steadily with the increase of red clay

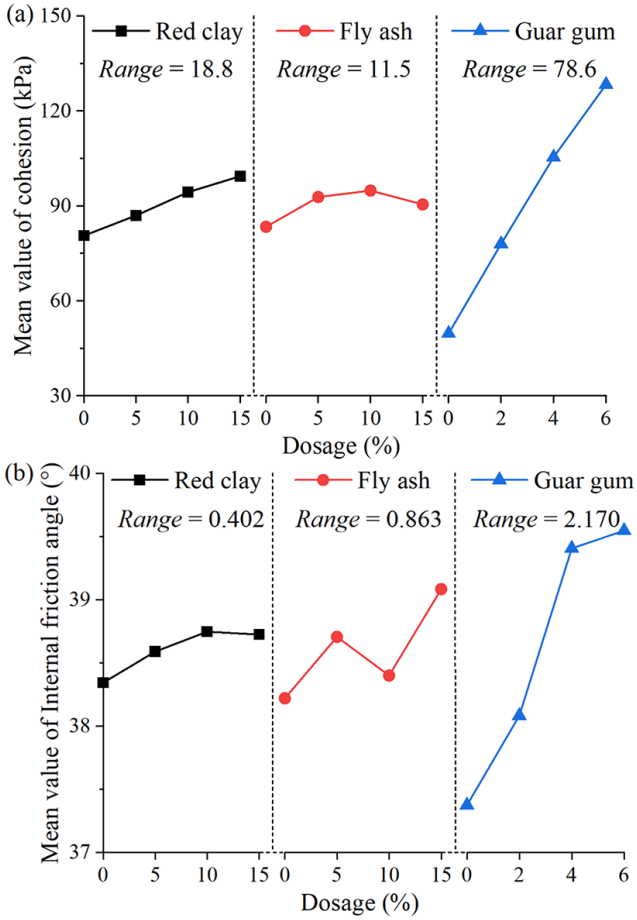

Fig. 12 Mean value of the test indexes at each dosage level: (a) cohesion, and (b) internal friction angle

and guar gum dosage, while the mean value of the internal friction angle tended to stabilise after the increase. With increased fly ash dosage, the cohesion showed a trend of increasing and then decreasing, while the internal friction angle did not change significantly. Range analysis indicated that the guar gum dosage has the greatest effect on both cohesion and internal friction angle, at 78.6 kPa and 2.17°, respectively. Variance analysis (Table 5) shows red clay and guar gum significantly affect cohesion, while fly ash does not, and the significant effect factor of internal friction angle is only the guar gum dosage. It can be seen that guar gum dosage has the most significant effect on shear strength indexes, red clay dosage has a significant effect on cohesion only, and fly ash dosage has less effect. Considering the dosage of modified materials and the shear strength indexes, it is suggested to use 10% red clay, 5% fly ash and 4% guar gum modified CM-SRM.

3.3 Composite modification mechanisms

To investigate the composite modification mechanisms of three modified materials on CM-SRM, micrographs of unmodified samples and composite modified samples at the recommended dosage were obtained using scanning electron microscopy (Fig. 13). The test method is the same as that described in reference [11, 13].

It can be observed that the unmodified CM-SRM primarily exhibits a platy and layered structure formed by the stacking of CM particles, with numerous microcracks and isolated plate particles, resulting in a relatively loose overall structure. After composite modification, the CM-SRM exhibits a large number of dense agglomerates and spherical fly ash particles, with the particles interconnected through a gel network, enhancing their bonding. Some pores are also filled with fly ash and associated binding products, demonstrating improved structural integrity.

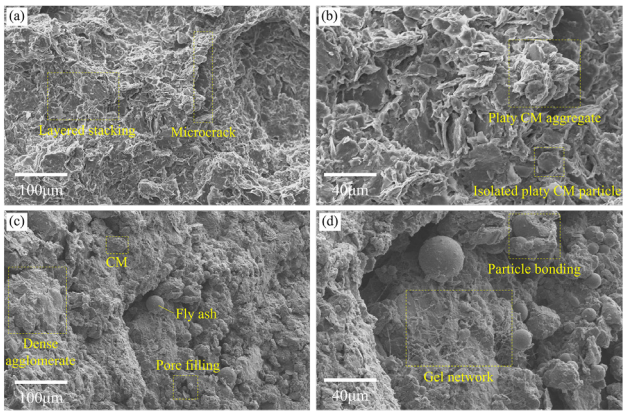

Fig. 13 SEM images of CM-SRM before and after modification: (a) unmodified CM-SRM (200x), (b) unmodified CM-SRM (500x), (c) suggested dosage of composite modified CM-SRM (200x), and (d) suggested dosage of composite modified CM-SRM (500x)

Table 5 Variance analysis results for cohesion and internal friction angle

Test index	Factor	Deviation sums of square	Mean square	*F* value	*p* value
Cohesion	Red clay dosage	814.714	271.571	10.016	0.009
	Fly ash dosage	298.950	99.650	3.675	0.082
	Guar gum dosage	13885.725	4628.575	170.715	0.001
Internal friction angle	Red clay dosage	0.410	0.137	0.197	0.895
	Fly ash dosage	1.713	0.571	0.822	0.528
	Guar gum dosage	13.238	4.413	6.349	0.027

Based on the above test results, combined with relevant literature and material properties, the composite modification mechanisms of red clay, fly ash, and guar gum on CM-SRM can be inferred (Fig. 14). It mainly includes the following three aspects:

(1) Binding and filling effects

The CM-SRM solution is weakly alkaline [13], which promotes the pozzolanic reaction between the active SiO_2 and Al_2O_3 in fly ash and red clay with $Ca(OH)_2$ (Fig. 14(b)), producing hydrated products with binding properties such as calcium silicate hydrate (C-S-H) and calcium aluminate hydrate (C-A-H) [11, 38, 39]. These hydration products can bind nearby particles to form structurally dense aggregates, enhancing the material's overall integrity. Meanwhile, dispersed fly ash and red clay particles fill the initial pores of the CM-SRM matrix [39] (Fig. 13(c)), and through pozzolanic reactions and the inherent binding properties of red clay, strengthen the connection between the fillers and the matrix [40], forming a more stable structure (Fig. 14(a)).

However, aggregation may occur when the dosage of fly ash and red clay is too high, reducing the activity and dispersibility of SiO_2 and Al_2O_3, thereby inhibiting the pozzolanic reaction and leading to a reduction in the strength improvement of CM-SRM (Fig. 12(a)).

(2) Cation exchange

Red clay is mainly composed of minerals such as kaolinite and hematite, which possess high specific surface areas and strong cation exchange capacities [35, 41]. Addition of red clay increases the concentration of free cations such as K^+, Ca^{2+}, and Mg^{2+} in the system, which then undergo cation exchange with Na^+ in CM-SRM (Fig. 14(c)). The cation exchange process will result in a reduction in the thickness of the double layer and bound water film, thereby enhancing the interparticle bonding force [11]. Adsorption of cations on the particle surface will also reduce the interparticle spacing, bringing the particles into closer contact. At the same time, the OH^- released during the reaction process will increase the alkalinity of the environment, providing a favorable environment for volcanic ash reactions.

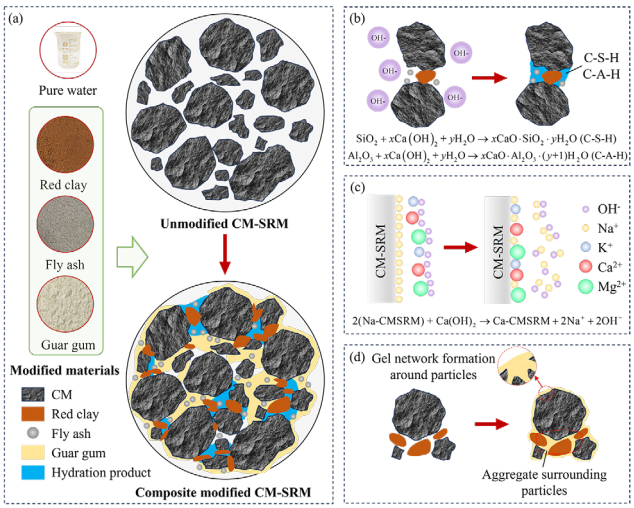

Fig. 14 Composite modification mechanisms: (a) overall structural changes, (b) pozzolanic reaction, (c) cation exchange, and (d) gel aggregation

(3) Gel aggregation

Guar gum possesses strong water absorption and expansion capabilities, as well as molecular entanglement properties [28, 42]. When mixed with water, it generates a large number of positively charged active functional groups. These functional groups can attract negatively charged clay minerals, forming stable aggregates [43]. Additionally, the hydrogels formed by guar gum dissolution can bind to mineral surfaces via hydrogen bonding and van der Waals forces, enveloping the CM-SRM particle surfaces to form a three-dimensional gel network structure (Fig. 13(d)), thereby enhancing cohesive forces among aggregating nearby particles [44, 45].

The combined effects of the above three effects enable the composite modified CM-SRM to exhibit superior strength properties.

4 Strength evaluation method for CM-SRM considering modified material dosage

Current evaluation method s for the strength of soil-rock mixtures mostly focusses on high-quality fillers, while poor fillers typically require modification to improve their properties in engineering. To promote the application of modified CM-SRM in engineering, this study establishes a strength evaluation method for CM-SRM considering the dosage of modified materials based on the results of orthogonal tests. The method's validity is verified by comparing the evaluation results with the test data.

4.1 Modifying the theoretical equations for UCS

The lateral pressure of the specimen under the unconfined condition is 0 (i.e., the confining pressure $\sigma_3 = 0$ kPa), which belongs to a special case in the triaxial test. According to the ultimate equilibrium condition at a point in soil, the theoretical value of UCS, q_u is obtained as:

$$q_u = \sigma_1 = 2c\tan\left(45 + \frac{\varphi}{2}\right), \tag{1}$$

where c and φ are the cohesion and internal friction angle of the specimen, respectively, and σ_1 is the axial stress to

which the specimen is subjected. The theoretical value of UCS was calculated by substituting the shear strength indexes of each specimen (Fig. 11) into Eq. (1), and the results are shown in Fig. 15.

Comparison between the UCS test results and the theoretical calculation results reveals a maximum deviation percentage of 40.7% and an approximately linear correlation. Accordingly, Eq. (1) is corrected based on the UCS test results, and the corrected UCS theoretical value Q_u is calculated by linear fitting as:

$$Q_u = a\left[2c\tan\left(45+\frac{\varphi}{2}\right)\right]+b\,, \tag{2}$$

where a and b are fitting parameters, in this study $a = 0.94$ and $b = 118.32$. The maximum percentage deviation between the corrected theoretical and experimental values of UCS is only 7.6%, which can be used to calculate the UCS through the shear strength indexes.

4.2 Strength evaluation methods for composite modification CM-SRMs

Firstly, the multiple linear regression models were used to establish the evaluation equations of shear strength indexes,

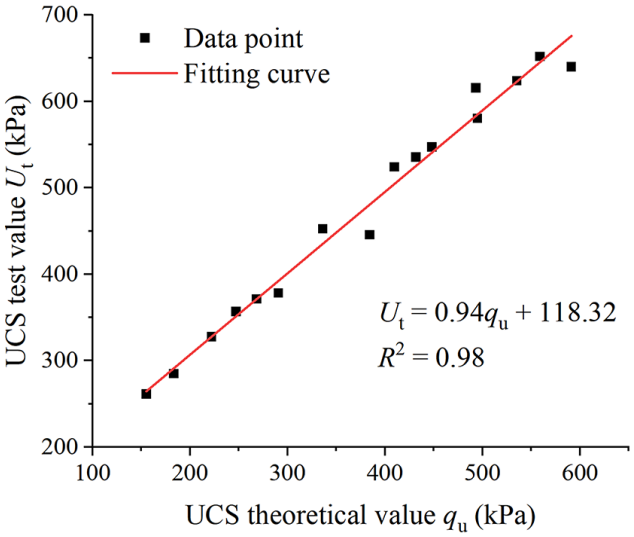

Fig. 15 Relationship between theoretical and test values of UCS

and the equations were divided based on whether interactions between factors were considered. The evaluation results are shown in Table 6. Comparing both linear models, it is known that considering the interaction between factors has limited improvement on the evaluation accuracy, but it adds more fitting parameters, so the interaction between factors can be ignored. The correlation coefficient R^2 of the cohesion evaluation equation is greater than 0.97, which shows a good evaluation effect, while the R^2 of the internal friction angle evaluation equation is only 0.64, which shows a less evaluation effect. By comparing coefficients of various dosages, the influence degree of different factors on the shear strength indexes can also be assessed, and the results reflected through Table 6 are consistent with the orthogonal analyses.

Compared to linear regression models, nonlinear regression models are able to capture the non-linear relationships within data more effectively, thereby providing a more accurate evaluation ability. To determine the optimal evaluation equation, this study compared the non-linear and linear evaluation equations for the shear strength indexes. Orthogonal analysis results (Fig. 12) show that cohesion mean value generally matches a linear relationship with red clay and guar gum dosage, while it matches a quadratic relationship with fly ash dosage. The internal friction angle shows a quadratic relationship with the dosage of red clay and guar gum, and a cubic relationship with the fly ash dosage. Subsequently, fitting the data by the corresponding functions (see Table 7), the correlation coefficients of each regression equation exceeded 0.85. Further linear combination of these regression curves yielded the non-linear evaluation equation for CM-SRM cohesion and internal friction angle based on dosage of modified materials as:

$$c = Ax_2^2 + Bx_1 + Cx_2 + Dx_3 + E \tag{3}$$

$$\varphi = Fx_2^3 + (Gx_1 + Hx_2 + Ix_3 + 1)^2 + J\,, \tag{4}$$

where, A, B, C, D, E, F, G, H, I, J are undetermined coefficients. The test results of shear strength indexes of the specimens can be substituted into Eqs. (5) and (6) to solve the undetermined coefficients, and the results are:

Table 6 Multiple linear regression equation

Evaluation index	Consideration of factor interactions	Evaluation equation	R^2
Cohesion c	No	$c = 1.27\,x_1 + 0.46\,x_2 + 13.16\,x_3 + 37.84$	0.97
	Yes	$c = 1.23\,x_1 + 0.40\,x_2 + 15.10\,x_3 - 0.01\,x_1\,x_2 - 0.21\,x_1\,x_3 - 0.21\,x_2\,x_3 + 0.05\,x_1\,x_2\,x_3 + 37.88$	0.98
Internal friction angle φ	No	$\varphi = 0.03\,x_1 + 0.05\,x_2 + 0.39\,x_3 + 36.89$	0.62
	Yes	$\varphi = 0.12\,x_1 + 0.19\,x_2 + 0.88\,x_3 - 0.01\,x_1\,x_2 - 0.04\,x_1\,x_3 - 0.05\,x_2\,x_3 + 36.02$	0.64

Table 7 Regression equation of modified material dosage and shear strength indexes

Evaluation index	Factor	Evaluation equation	R^2
Cohesion c	Red clay dosage	$c = 1.27\,x_1 + 80.81$	0.99
	Fly ash dosage	$c = -0.14\,x_{22} + 2.54\,x_2 + 83.42$	0.99
	Guar gum dosage	$c = 13.16\,x_3 + 50.88$	0.99
Internal friction angle φ	Red clay dosage	$\varphi = -0.003\,x_{12} + 0.066\,x_1 + 38.340$	0.98
	Fly ash dosage	$\varphi = 0.002\,x_{23} - 0.051\,x_{22} + 0.295\,x_2 + 36.890$	0.99
	Guar gum dosage	$\varphi = -0.035\,x_{32} + 0.604\,x_3 + 37.285$	0.85

$$\begin{cases} A = -0.13, B = 1.27, C = 2.54, \\ D = 13.16, E = 34.39 \\ F = 0.0002, G = 0.0070, H = -0.0039, \\ I = 0.1330, J = 36.2100 \end{cases} \tag{5}$$

Finally, the non-linear evaluation equation for the cohesion and internal friction angle of CM-SRM is obtained as:

$$c = -0.13x_2^2 + 1.27x_1 + 2.54x_2 + 13.16x_3 + 34.39 \quad R^2 = 0.98 \tag{6}$$

$$\varphi = 0.0002x_2^3 + \begin{pmatrix} 0.0070x_1 - 0.0039x_2 \\ +0.1330x_3 + 1 \end{pmatrix}^2 + 36.2100 \quad R^2 = 0.68 \tag{7}$$

4.3 Models comparison

The evaluation results of shear strength indexes for linear and non-linear equations are shown in Fig. 16. A comparison of the two cohesion evaluation equations (Fig. 16(a)) reveals that, while the non-linear equation has a small mean of error percentage, its maximum error percentage exceeds 10%. For the evaluation equation of internal friction angle (Fig. 16(b)), the percentage error of both methods is less than 4%, and the comparison of the mean of percentage error and the correlation coefficient shows that the non-linear equation is more accurate. Hence, the linear equation is chosen to evaluate the cohesion, and the non-linear equation is chosen to evaluate the internal friction angle.

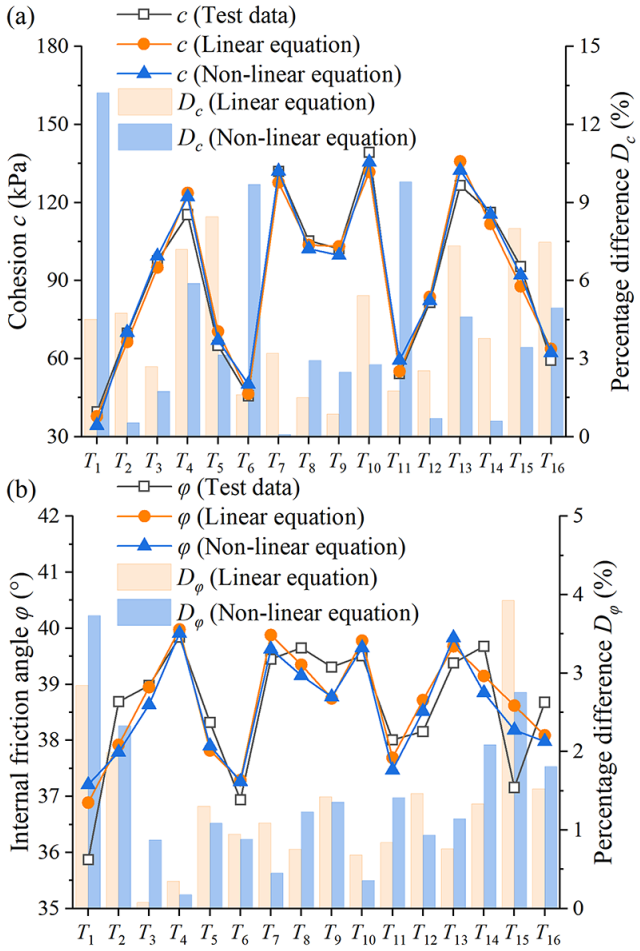

Fig. 16 Comparison of evaluated and tested values of shear strength indexes: (a) cohesion, and (b) internal friction angle

After determining the evaluation equations for cohesion and internal friction angle, the shear strength τf of composite modified CM-SRM under different normal stress conditions can be obtained by combining with Mohr-Coulomb criterion, which is calculated as:

$$\tau_f = 1.27x_1 + 0.46x_2 + 13.16x_3 + 37.84 + \sigma \tan\left[0.0002x_2^3 + \left(0.0070x_1 - 0.0039x_2 + 0.1330x_3 + 1\right)^2 + 36.2100\right] \tag{8}$$

$$Q_u = 118.32 + 0.94\left\{2\begin{pmatrix} 1.27x_1 + 0.46x_2 \\ +13.16x_3 + 37.84 \end{pmatrix} \times \tan\left(45 + \frac{\left[0.0002x_2^3 + \begin{pmatrix} 0.0070x_1 - 0.0039x_2 \\ +0.1330x_3 + 1 \end{pmatrix}^2 + 36.2100\right]}{2}\right)\right\} \tag{9}$$

The UCS for each modification scheme was calculated using Eq. (8) and compared with the test values, as shown in Fig. 17. The evaluated UCS closely matches the test values, with a maximum percentage difference of about 6.5% and a minimum value of about 0.1%, indicating that this equation provides a high degree of accuracy in evaluating the UCS of composite modified CM-SRM. In practical engineering, Eq. (8) or Eq. (9) can be selected to calculate the shear strength or UCS of composite modified CM-SRM based on the stress conditions of the filler, so as to provide a reference for embankment structural design.

5 Conclusions

In this study, the strength properties of CM-SRM under different modification schemes were systematically analysed and a method for the evaluation of shear strength parameters was proposed. The main conclusions are as follows:

1. The failure modes of modified CM-SRM mainly include single-shear, single-shear-bulk, double-shear and double-shear-bulk etc., which are significantly affected by the fly ash and guar gum dosage and the confining pressure.
2. Whether modified or not, CM-SRM exhibited strain softening behaviour. The addition of modifiers weakened the softening effect, with fly ash having the most significant effect. Additionally, the UCS and cohesion of modified CM-SRM are significantly increased, while the internal friction angle changes little.
3. Orthogonal analyses showed that all three modifier dosages had a significant effect on UCS, with guar gum having the strongest effect, followed by red clay, and fly ash having the smallest effect. Guar gum has a significant effect on both cohesion and internal friction angle, while red clay mainly affects cohesion and fly ash has a weak effect on shear strength index.
4. Linear and non-linear evaluation equations for shear strength index were developed respectively, where the linear model is more suitable for cohesion evaluation and the non-linear model is more accurate for internal friction angle evaluation. The accuracy of the proposed strength evaluation method was proved to be high.
5. Red clay, fly ash, and guar gum primarily improve the structure of composite modified CM-SRM through binding and filling effects, cation exchange, and gel aggregation, thereby enhancing its mechanical properties. Combining mechanical properties and economy, The suggested dosage combination is 10% red clay, 5% fly ash, and 4% guar gum.

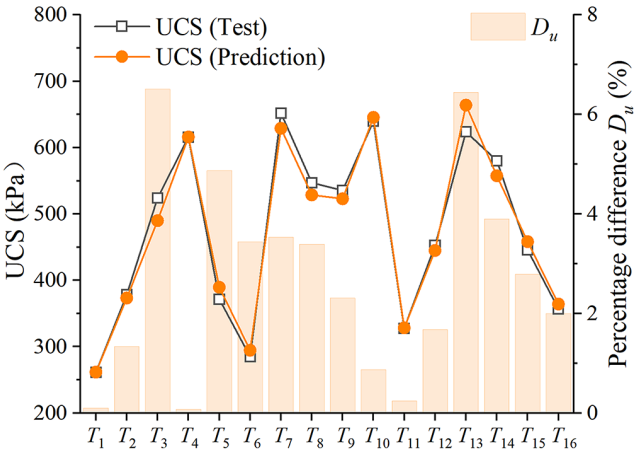

Fig. 17 Relationship between evaluated and tested values of UCS

This study mainly evaluates the performance of CM-SRM based on laboratory conditions, and its long-term durability, environmental friendliness, and field-use performance should be further investigated in the future. In addition, its reliability under cyclic loading and freeze-thaw cycle conditions should be investigated to verify its applicability in different climatic environments.

Acknowledgements

This work was supported by the National Natural Science Foundation of China (52378440, 42477143); the Key Science and Technology Program in the Transportation Industry (2022-MS1-032, 2022-MS5-125); the Natural Science Foundation of Hunan Province (2023JJ10045); the Guangxi Key Research and Development Program (AB23075184); the Program of China Scholarship Council (202408430148); and the Postgraduate Scientific Research Innovation Project of Hunan Province (CX20240764).

References

[1] Zeng, L., Yu, H. C., Liu, J., Gao, Q. F., Bian, H. B. "Mechanical behaviour of disintegrated carbonaceous mudstone understress and cyclic drying/wetting", Construction and Building Materials, 282, 122656, 2021. https://doi.org/10.1016/j.conbuildmat.2021.122656

[2] Zeng, L., Yu, H. C., Qiu, J., Luo, J. T., Liu, J., Gao, Q. F., Zhang, H. R. "Pore characteristics and microscopic damage mechanism of disintegrated carbonaceous mudstone exposed to dry-wet cycles", Construction and Building Materials, 433, 136774, 2024. https://doi.org/10.1016/j.conbuildmat.2024.136774

[3] Rahman, A. M., Imteaz, M. A., Arulrajah, A., Piratheepan, J., Disfani, M. M. "Recycled construction and demolition materials in permeable pavement systems: Geotechnical and hydraulic characteristics", Journal of Cleaner Production, 90, pp. 183–194, 2015. https://doi.org/10.1016/j.jclepro.2014.11.042

[4] Fu, H. Y., Xue, C. W., Wen, W., Yang, Q. Y., Chen, L. "Research on the road performance of carbonaceous mudstone soil-rock mixtures under multifactor influence", KSCE Journal of Civil Engineering, 28(4), pp. 1227–1237, 2024. https://doi.org/10.1007/s12205-024-1005-8

[5] Zha, H. Y., Fu, H. Y., Zeng, L., Zhu, X. B., Jia, C. K. "Use of sodium alginate as a novel cementitious material to improve the engineering properties of disintegrated carbonaceous mudstone", Bulletin of Engineering Geology and the Environment, 81(10), 431, 2022. https://doi.org/10.1007/s10064-022-02936-0

[6] Orioli, M. A., Costa, W. G. S., Baldin, C. R. B., Muñoz, Y. O., Izzo, R. L. D. S. "Silty soil resilient modulus stabilised with cement and recycled aggregate", International Journal of Pavement Engineering, 25(1), 2378334, 2024. https://doi.org/10.1080/10298436.2024.2378334

[7] Haq, M., Khan, M. A., Ali, S., Ali, K., Yusuf, M., Kamyab, H., Irshad, K. "Enhancing clayey soil performance with lime and waste rubber tyre powder: Mechanical, microstructural, and statistical analysis", Environmental Research, 256, 119217, 2024. https://doi.org/10.1016/j.envres.2024.119217

[8] Ruan, S., Liu, L., Zhu, M., Shao, C., Xie, L., Hou, D. "Application of desulfurization gypsum as activator for modified magnesium slag-fly ash cemented paste backfill material", Science of the Total Environment, 869, 161631, 2023. https://doi.org/10.1016/j.scitotenv.2023.161631

[9] Khadka, S. D., Jayawickrama, P. W., Senadheera, S., Segvic, B. "Stabilization of highly expansive soils containing sulfate using metakaolin and fly ash based geopolymer modified with lime and gypsum", Transportation Geotechnics, 23, 100327, 2020. https://doi.org/10.1016/j.trgeo.2020.100327

[10] Wu, Z., Deng, Y., Liu, S., Liu, Q., Chen, Y., Zha, F. "Strength and micro-structure evolution of compacted soils modified by admixtures of cement and metakaolin", Applied Clay Science, 127–128, pp. 44–51, 2016. https://doi.org/10.1016/j.clay.2016.03.040

[11] Zeng, L., Yu, H. C., Gao, Q. F., Bian, H. B. "Mechanical behavior and microstructural mechanism of improved disintegrated carbonaceous mudstone", Journal of Central South University, 27(7), pp. 1992–2002, 2020. https://doi.org/10.1007/s11771-020-4425-8

[12] Amulya, S., Shankar, A. U. R., Praveen, M. "Stabilisation of lithomargic clay using alkali activated fly ash and ground granulated blast furnace slag", International Journal of Pavement Engineering, 21(9), pp. 1114–1121, 2018. https://doi.org/10.1080/10298436.2018.1521520

[13] Zeng, L., Yu, H. C., Gao, Q. F., Zha, H. Y., Zu, Y. X., Bian, H. B. "Road performance and modification mechanisms of disintegrated carbonaceous mudstone modified with gum Arabic", China Journal of Highway and Transport, 36(10), pp. 42–54, 2023. https://doi.org/10.19721/j.cnki.1001-7372.2023.10.004

[14] Chen, C. Y., Fu, H. Y., Gao, Q. F., Zeng, L., Jia, C. K. "Polyurea reinforcement of disintegrated mudstone embankments and the underlying mechanism", Transportation Geotechnics, 37, 100874, 2022. https://doi.org/10.1016/j.trgeo.2022.100874

[15] González-Aviña, J. V., Hosseinpoor, M., Yahia, A., Durán-Herrera, A. "New biopolymers as viscosity-modifying admixtures to improve the rheological properties of cement-based materials", Cement and Concrete Composites, 146, 105409, 2024. https://doi.org/10.1016/j.cemconcomp.2023.105409

[16] Mahamaya, M., Das, S. K., Reddy, K. R., Jain, S. "Interaction of biopolymer with dispersive geomaterial and its characterization: An eco-friendly approach for erosion control", Journal of Cleaner Production, 312, 127778, 2021. https://doi.org/10.1016/j.jclepro.2021.127778

[17] Zhang, R., Lu, Z., Liu, J., Zhao, Y., Feng, Y. N. "Physical and mechanical properties of saline soil stabilized by combined slag, fly ash and polyacrylamide", Rock and Soil Mechanics, 45(S1), pp. 123–132, 2024.

[18] Fu, H. Y., Zha, H. Y., Pan, H. Q., Zeng, L., Liu, J. "Experimental study on water stability and scour resistance of biopolymer modified disintegrated carbonaceous mudstone", Journal of Central South University (Science and Technology), 53(7), pp. 2633–2644, 2022.

[19] Fu, H. Y., Zha, H. Y., Zeng, L., Chen, C. Y., Jia, C. K. Bian, H. B. "Research progress on ecological protection technology of highway slope: status and challenges", Transportation Safety and Environment, 2(1), pp. 3–17, 2020. https://doi.org/10.1093/tse/tdaa006

[20] Chen, C. Y., Fu, H. Y., Chen, Y. Y. "Disintegration behavior and its grading entropy characterization of polyurea modified graded carbonaceous mudstone under loading and drying-wetting cycles", Construction and Building Materials, 411, 134435, 2024. https://doi.org/10.1016/j.conbuildmat.2023.134435

[21] Yang, Q. Y., Wen, W., Zeng, L., Fu, H. Y., Gao, Q. F., Chen, L., Bian, H. B. "Road performance and prediction model for carbonaceous mudstone soil-rock mixtures under wet-dry cycles", Road Materials and Pavement Design, 25(8), pp. 1790–1808, 2024. https://doi.org/10.1080/14680629.2023.2278146

[22] Yang, Q. Y., Wen, W., Zeng, L., Fu, H. Y., Chen, L., Bian, H. B., Zhang, H. R. "Research on the dynamic resilience characteristics of carbonaceous mudstone soil-rock mixture under wet-dry cycles", Bulletin of Engineering Geology and the Environment, 83(7), 298, 2024. https://doi.org/10.1007/s10064-024-03789-5

[23] Zeng, L., Li, Fan., Gao, Q. F., Bian, H. B. "Effect of initial gravimetric water content and cyclic wetting-drying on soil-water characteristic curves of disintegrated carbonaceous mudstone", Transportation Safety and Environment, 1(3), pp. 230–240, 2019. https://doi.org/10.1093/tse/tdz018

[24] Ministry of Transport of the People's Republic of China "JTG 3430-2020, Test methods of soils for highway engineering", Ministry of Transport of the People's Republic of China, Beijing, China, 2020.

[25] Zeng, L., Yu, H. C., Gao, Q. F., Liu, J., Liu, Z. H. "Evolution of tensile properties of compacted red clay under wet and dry cycles", KSCE Journal of Civil Engineering, 26(2), pp. 606–618, 2022. https://doi.org/10.1007/s12205-021-0527-6

[26] Gao, Q. F., Yu, H. C., Zeng, L., Huang, Y. X. "Characterization of water retention behavior of cracked compacted lateritic soil exposed to wet-dry cycles", Bulletin of Engineering Geology and the Environment, 82(2), 61, 2023.
https://doi.org/10.1007/s10064-023-03089-4

[27] Amiri, A., Toufigh, M. M., Toufigh, V. "Stabilisation of organic soils with alkali-activated binders", International Journal of Pavement Engineering, 24(2), 2104844, 2023.
https://doi.org/10.1080/10298436.2022.2104844

[28] Fu, H. Y., Yu, G. T., Gao, Q. F., Zeng, L., Cao, S. P. "Crack resistance and strength properties of red clay modified with lignocellulose and guar gum", KSCE Journal of Civil Engineering, 27(10), pp. 4152–4162, 2023.
https://doi.org/10.1007/s12205-023-2005-9

[29] Ghosh, T., Katiyar, V. "Nanochitosan functionalized hydrophobic starch/guar gum biocomposite for edible coating application with improved optical, thermal, mechanical, and surface property", International Journal of Biological Macromolecules, 211, pp. 116–127, 2022.
https://doi.org/10.1016/j.ijbiomac.2022.05.079

[30] Zhang, J. H., Peng, J. H., Zeng, L., Li, J., Li, F. "Rapid estimation of resilient modulus of subgrade soils using performance-related soil properties", International Journal of Pavement Engineering, 22(6), pp. 732–739, 2019.
https://doi.org/10.1080/10298436.2019.1643022

[31] Fu, H. Y., Yu, X. Y., Liu, J., Zeng, L., Chen, X. W. "Study of the strength properties and micromechanisms of nano-Al_2O_3-modified predisintegrated carbonaceous mudstone based on orthogonal design", Quarterly Journal of Engineering Geology and Hydrogeology, 56(4), 018, 2023.
https://doi.org/10.1144/qjegh2023-018

[32] Fu, H. Y., Yang, Q. Y., Zeng, L., Gao, Q. F., Wen, W., Chen, L. "Dynamic resilient characteristics of disintegrated carbonaceous mudstoneunder the influence of multiple factors", China Civil Engineering Journal, 57(2), pp. 117–128, 2024.
https://doi.org/10.15951/j.tmgcxb.22101023

[33] Basu, A., Mishra, D. A., Roychowdhury, K. "Rock failure modes under uniaxial compression, Brazilian, and point load tests", Bulletin of Engineering Geology and the Environment, 72(3), pp. 457–475, 2013.
https://doi.org/10.1007/s10064-013-0505-4

[34] Labuz, J. F., Zang, A. "Mohr-Coulomb failure criterion", Rock Mechanics and Rock Engineering, 45(6), pp. 975–979, 2012.
https://doi.org/10.1007/s00603-012-0281-7

[35] Gao, Q. F., Wu, X. Y., Zeng, L., Yu, H. C., Yu, H. "Mechanisms behind wetting self-healing behavior and its influence on the strength of lateritic soil", China Journal of Highway and Transport, 37(6), pp. 157–168, 2024.
https://doi.org/10.19721/j.cnki.1001-7372.2024.06.013

[36] Karami, H., Pooni, J., Robert, D., Costa, S., Li, J., Setunge, S. "Use of secondary additives in fly ash based soil stabilization for soft subgrades", Transportation Geotechnics, 29, 100585, 2021.
https://doi.org/10.1016/j.trgeo.2021.100585

[37] Rasti, A., Adarmanabadi, H. R., Pineda, M., Reinikainen, J. "Evaluating the effect of soil particle characterization on internal friction angle", American Journal of Engineering and Applied Sciences, 14(1), pp. 129–138, 2021.
https://doi.org/10.3844/ajeassp.2021.129.138

[38] Barman, D., Dash, S. "Stabilization of expansive soils using chemical additives: A review", Journal of Rock Mechanics and Geotechnical Engineering, 14(4), pp. 1319–1341, 2022.
https://doi.org/10.1016/j.jrmge.2022.02.011

[39] Guan, Y., Zhang, Z., Zhang, X., Zhu, J., Zhou, W., Huang, Q., Zhang, Y. "Effect of superabsorbent polymer on mechanical properties of cement stabilized base and its mechanism", Construction and Building Materials, 2(1), pp. 58–68, 2020.
https://doi.org/10.1093/tse/tdaa001

[40] Liu, Y., Gu, F., Zhou, H., Li, Q., Shang, S. "Study on the performance and reaction mechanism of alkali-activated clay brick with steel slag and fly ash", Construction and Building Materials, 411, 134406, 2023.
https://doi.org/10.1016/j.conbuildmat.2023.134406

[41] Yu, H. C., Zeng, L., Wu, X. Y., Gao, Q. F., Bian, H. B., Luo, J. T., Chen, J. C., Zhang, H. R. "Classification of cracking potential for clayey soils based on cyclic wet-dry tests", Environmental Earth Sciences, 84(8), 198, 2025.
https://doi.org/10.1007/s12665-025-12210-7

[42] Banne, S. P., Kulkarni, S., Baldovino, J. A. "Effect of guar gum content on the mechanical properties of laterite soil for subgrade soil application", Polymers, 16(15), 2022, 2024.
https://doi.org/10.3390/polym16152202

[43] Kumar, S., Yadav, B. D., Raj, R. "A review on the application of biopolymers (xanthan, agar and guar) for sustainable improvement of soil", Discover Applied Sciences, 6(8), 393, 2024.
https://doi.org/10.1007/s42452-024-06087-7

[44] Sujatha, E. R., Saisree, S. "Geotechnical behaviour of guar gum-treated soil", Soils and Foundations, 59(6), pp. 2155–2166, 2019.
https://doi.org/10.1016/j.sandf.2019.11.012

[45] Xu, X., Chu, H., Wang, Q., Li, J., Yuan, X., Niu, C., Lei, H., Yu, Z. "Dispersion, mechanical, hydrophysical properties and mechanistic analysis of improved dispersive soil using guar gum", Bulletin of Engineering Geology and the Environment, 84(1), 56, 2025.
https://doi.org/10.1007/s10064-024-04082-1